ISSN: 0974-2115
www.jchps.com Journal of Chemical and Pharmaceutical Sciences

Structural and dielectric properties of Ni^{+2} doped Chromium Ferrite by Solution Combustion method

Abdul Khader S[1*], Mohamed Shariff S[1], Firdous Nayeem[1], Basavaraja J[1], Madanakumara H[2], Thyagaraj M S[3]

[1]Department of Physics, Govt. Science College, Chitradurga-577501, Karnataka, India
[2]Department of Physics, Dr. Ambedkar Institute of Technology, Bangalore-560056, India
[3]Department of Physics, HEA Polytechnic, Bangalore-560037, India
[*]**Corresponding author: E-Mail: Khadersku@gmail.com, Ph: 919980787658**

ABSTRACT

Nickel doped Chromium ferrite nanoparticles having the basic composition $Ni_xCr_{1-x}Fe_2O_4$(x=0, 0.25, 0.5, 0.75, 1) were synthesized using solution combustion method. The structural and dielectric properties of these samples, which are sintered at 800^0C were studied. The structure and phase of the synthesized samples were probed by X-ray diffraction (XRD) studies. The peaks observed in the XRD patterns indicate single phase spinel cubic structure for the synthesized ferrite samples. Surface morphology of the samples has been studied using FESEM. The dielectric constant (ε') and dielectric loss tangent (tan δ) of nanocrystalline chromium ferrites were investigated as a function of frequency and Ni^{+2} concentration at room temperature over the frequency range 100 Hz to 1 MHz using Hioki LCR Hi-Tester-3250. Frequency dependence of ε' and tan δ, is in accordance with the Maxwell-Wagner type interfacial polarization. The electrical conductivity (σ_{ac}) is deduced from the measured dielectric data, and found that the electrical conduction mechanism in the present $Ni_xCr_{1-x}Fe_2O_4$ nano-ferrites are in conformity with the electron hopping model.

KEY WORDS: combustion, dielectric properties, a.c conductivity, nanoferrites.

1. INTRODUCTION

Nano-crystalline magnetic oxides with cubic spinel structure are extensively studied, because of their excellent tunable electrical and magnetic properties (Yao, 2007). Using low temperature synthesis techniques such as combustion technique they can be synthesized even at room temperature. By doping with different metallic ions into spinel lattice their properties can be modified and can be used as functional materials (Hankare, 2011).

Magnetic spinel oxides with formula $MO.Fe_2O_3$ or MFe_2O_4, where 'M' is the divalent metal ion. The crystalline structure of a magnetic oxide (ferrite) can be considered as, an interlocking network of positively charged metal ions and negatively charged divalent oxygen ions (Brabers, 1995). In spinel ferrites, the doping of different metal ions with different valencies for the two types of lattice sites depends on the ionic radii of the substituted ions, the size of interstices, orbital preference for the specific coordination and the temperature (Akhtar, 2014; 2011).

These substituted divalent and trivalent metal ions such as Fe^{+3}, Fe^{+2}, Ni^{+2}, Co^{+2} and Mn^{+2} into the crystal lattice of magnetic spinels, one can provide the unaired electron spins and contribute towards the magnetic moment of the spinel, and represent the ferromagnetic, anti-ferromagnetic and paramagnetic behavior of the compounds. For the synthesis of spinel magnetic oxides various approaches such as chemical, co-precipitation, sol-gel, spray pyrolysis, ion-exchange, micro-emulsion, ceramic method, hydrothermal, etc.

Compared to other mentioned synthesis techniques, Auto-combustion method has advantages such as it is very simple, fast and economical (Azadmanjari, 2007). Because of their imperative technological and bio-medical applications they are used in device applications like radiofrequency circuits, ferro-fluids, hyperthermia, transformer cores, microwave antennas, magnetic recording (Yue, 2000).

Since electrical and magnetic properties of ferrites are highly dependent on particle size. Nano-powders of the ferrites are preferred over their bulk counterpart. Nickel ferrite belongs to technologically important inverse spinel belonging to soft ferrites family (Gou, 2010; Azadmanjiri, 2008).

In our present study, samples with the basic composition $Ni_xCr_{1-x}Fe_2O_4$ (x=0, 0.25, 0.5, 0.75, 1) were synthesized using citrate gel solution- combustion method. This method is highly exothermic and self-propagating thermally-induced redox reaction of xerogel, which is obtained from aqueous solution containing desired metallic nitrates as oxidizer and organic fuel.

The oxidizer/fuel molar ratio needed for preparing a stoichiometric mixture is determined according to the valencies of the reacting elements in order to supply the relation of oxidizer/fuel equal to one (Gou, 2010). The metallic nitrates are preferred as precursors, because they are water-soluble, have low ignition temperatures and are easy to prepare. The aim of the present work is to investigate the mechanism of dielectric polarization and type of conduction in Ni-Cr ferrite system.

2. MATERIALS AND METHODS

The Ni-Cr ferrites having the general formula $Ni_xCr_{1-x}Fe_2O_4$ (where x=0.0, 0.25, 0.5, 0.75, 1.0) were prepared using Solution combustion method. The starting materials are Nickel Nitrate ($Ni(NO_3)_2.6H_2O$), Ferric Nitrate

($Fe(NO_3)_2.9H_2O$), Magnesium Nitrate ($Cr(NO_3)_3.9H_2O$, CA-Citric acid ($C_6H_8O_7.H_2O$). These metallic nitrates were mixed in deionized water with standard weight percentages according to their stoichiometry calculations. As per stoichiometric calculations, measured quantity of citric acid was taken as fuel and its aqueous solution was prepared. The molar ratio of metallic nitrates to CA was kept as 1:1. The aqueous solution containing redox mixture was taken in a silica crucible and is allowed in to a muffle furnace, in which the temperature was already maintained at a temperature of 500^0C. The mixture finally yields porous and fluffy voluminous powder. The fluffy material was ground to get ferrite powder. The as-burnt ash was calcined at 800^0C for 2 hours to get better crystallization and homogeneous cation distribution in the synthesized spinel and finally ground to get Ni-Cr ferrite nano powders.

The phase of the synthesized ferrite samples were probed by X-ray diffraction (XRD) studies using Bruker AXS D8 Advance X-ray diffractometer using Cu-Kα (λ=1.5406 A^0) radiation while operating at 40kV and at 30 mA in the 2θ range of 10^0-80^0. Surface morphology of the samples has been investigated using Field Emission Scanning Electron Microscope (FESEM, JEOL JSM 6700). The Capacitance, C_p and dissipation factor, tanδ as a function of frequency in the range 100 Hz-1 MHz was studied using a precision Hioki LCR meter-3250. The dielectric constants (ε') and dielectric loss factor (ε") were determined using the formulae (Shukla, 2008),

$$\varepsilon' = Ct/\varepsilon_0 A \quad (1)$$

$$\varepsilon'' = \varepsilon' \tan\delta \quad (2)$$

Where, t is the thickness and A the area of the pellet.

The ac conductivity, σ_{ac} was determined from the dielectric loss factor using a relation

$$\sigma_{ac} = \omega\, \varepsilon_0\, \varepsilon'' \quad (3)$$

Where, ε_0 is the vacuum permittivity and $\omega = 2\Pi f$ with f being frequency.

3. RESULTS AND DISCUSSION

Phase and Surface Morphology: The X-ray diffraction patterns of $Ni_xCr_{1-x}Fe_2O_4$ (where x=0.0, 0.25, 0.5, 0.75, 1.0) system are presented in Figure 1. The presence of (220), (311), (400), (422), (511) and (440) planes in the diffraction patterns confirms the cubic spinel structure for the sintered samples. The mean crystallite size was calculated from the most intense peak (311) using the Scherrer's formula, $t=k\lambda/\beta\cos\theta$; where t is crystallite size, β is the full width at half maximum (FWHM) of the peak (311) and k is instrumental constant (Azadmanjiri, 2008). The calculated average crystallite size is in the range of 30-63 nm. From inter-planar spacing (d) and miller indices (hkl) values (De Biasi, 2007; Atif, 2011), the lattice parameters were computed using and are shown in Table 1.

Microstructures were studied by placing the sintered samples under Scanning electron microscope. The micrographs of the synthesized and sintered samples are depicted in Fig. 2 (a-c), shows the surface morphology of pure $NiFe_2O_4$, $CrFe_2O_4$ and Ni^{+2} doped $CrFe_2O_4$. Optical micrographs show the uniform nature of the sintered particles with some agglomerated grainy structure. From surface morphology studies shows the presence of a large number of interfaces, which have a direct bearing on the dielectric properties of these ferrites.

Dielectric properties: The variation of dielectric constant (ε'), dielectric loss factor (ε") and ac conductivity (σ_{ac}) with frequency at 300K, for the pure chromium ferrite and Ni^{+2} doped chromium ferrite is shown in Fig.3. From the Fig.3 (a), it is clear that ε' decreases at lower frequencies and remains constant at higher frequencies. The variation of dielectric constant with applied frequency is due to charge transport relaxation. This dielectric dispersion is attributed to Maxwell (1929) and Wagner (1913) type interfacial polarization, as the dielectric constant is a combined effect of dipolar, electronic, ionic and interfacial polarizations. Since ionic polarization is expected to decrease with frequency, the measured ε' also decreases with frequency. The large values of ε' are related with space charge polarization at grain boundaries and inhomogeneous dielectric structure. These in homogeneties arise from preparation techniques, sintering temperature, impurities, grain structure and pores (Sutka, 2012; Kambale, 2010). By electron exchange between Fe^{+2} and Fe^{+3}, displacement of electrons takes place with respect to the applied field and these electrons determine polarization. The polarization decreases with increase in applied frequency and for further increase, the electric exchange between Fe^{+2}/Fe^{+3} cannot follow the alternating field hence reaches the constant value. From Figs. 3(a) and 3(b), the variation in ε" shows a similar behavior as seen for ε' versus frequency.

In order to understand the type of charge carriers and type of polarons responsible for conduction, ac conductivity, σ_{ac} were estimated as per $\sigma_{ac} = \omega\, \varepsilon_0\, \varepsilon''$, with ε_0 is the permittivity of free space and $\omega = 2\Pi f$.

The variation of σ_{ac} with frequency, f, is shown in Fig.3 (d) for all the five samples. The plots are linear for almost entire range of frequency except at very low frequency. Linear variation of σ_{ac} with frequency confirms that the electrical conduction in mixed spinel ferrite is because of the hopping of charge carriers between the localized states which confirms the small polaron type of conduction (Kambale, 2010; Vijaya Bhaskar, 2010). The conduction mechanism in doped ferrites can be explained based on hopping of charge carriers between Fe^{+2} and Fe^{+3} ions on octahedral lattice sites. The increase in the frequency of the applied field accelerates the hopping of charge carriers resulting an enhancement in the overall conduction process, thereby increasing the conductivity. At higher frequencies σ_{ac} remains constant because the hopping frequency of the charge carriers no longer follows the external

applied field variations and lags behind it. However, the slight decrease in conductivity at lower frequencies can be attributed to conduction by mixed polarons.

The numbers of ferrous (Fe^{+2}) ions play a key role in the mechanism of conduction and dielectric polarization. Small amount of Fe^{+2} ions increases electrical conductivity of a ferrite. The magnitude of electron exchange between Fe^{+2} and Fe^{+3} ions depends on the percentage concentration of Fe^{+2}/ Fe^{+3} present on the octahedral lattice i.e. on B-site. The Fe^{+2} ions concentration for a given ferrite material depends upon various material synthesis parameters e.g. sintering temperature atmosphere, cooling rate, type annealing etc. The magnitude of Fe^{+2} ions which takes part in the electron exchange contributes mainly for the conduction and polarization. Thus, the maximum value of ε' and σ_{ac} for x=0.5 sample may be mainly due to the enhanced formation of Fe^{+2} ions. The dielectric constant, ε' may thought to be directly proportional to electrical conductivity evidenced through plots Fig 3(a) and 3(d).

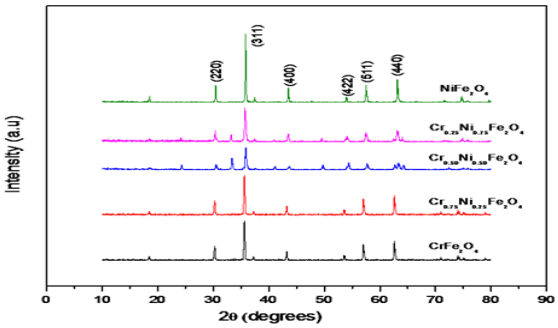

Figure.1. XRD diffractogram for Pure $CrFe_2O_4$ and Ni^{+2} doped $CrFe_2O_4$ samples

Table 1. Lattice constant and Crystallite Size values of $Ni_xCr_{1-x}Fe_2O_4$ samples

Sample	Crystallite size (nm)	Lattice constant 'a' (A^0)
$CrFe_2O_4$	63.16	8.3619
$Cr_{0.75}Ni_{0.25}Fe_2O_4$	60.15	8.3600
$Cr_{0.5}Ni_{0.5}Fe_2O_4$	35.99	8.3031
$Cr_{0.25}Ni_{0.75}Fe_2O_4$	30.11	8.3271
$NiFe_2O_4$	60.04	8.3081

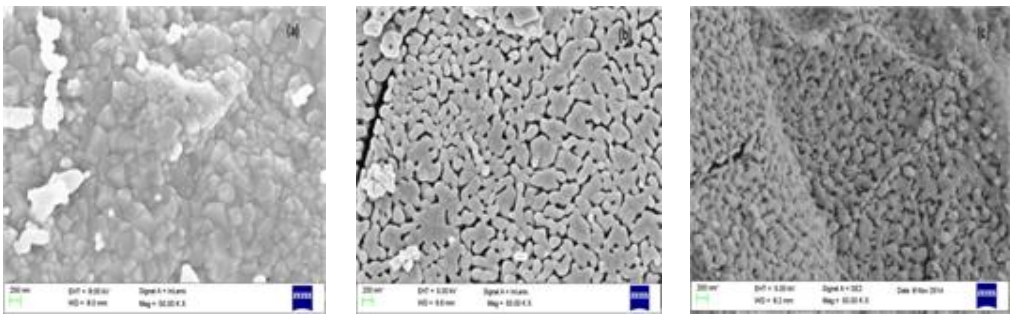

Fig.2. FESEM Micrographs for (a) NiFe2O4, (b) $CrFe_2O_4$ and (c) $Ni_{0.5}Cr_{0.5}Fe_2O_4$

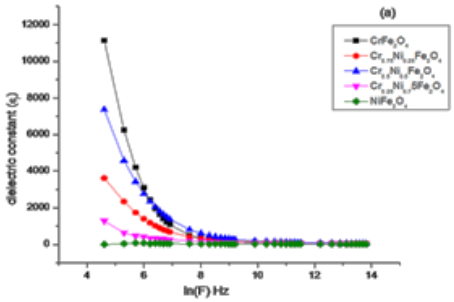

Figure.3. (a)Variation of ε' with ln(F) at RT.

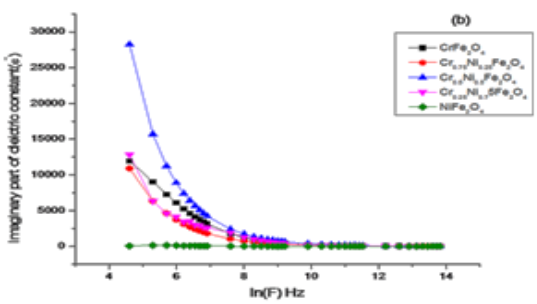

Figure.3. (b)Variation of ε'' with ln(F) at RT.

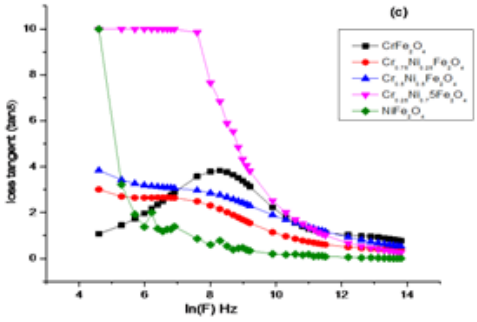

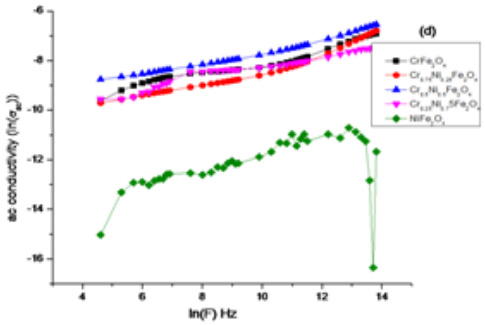

Figure.3(c) Variation of tanδ with ln(F) at RT. Figure.3(d) Variation of ln (σ_{ac}) with ln (F) at RT

4. CONCLUSIONS

The $Ni_xCr_{1-x}Fe_2O_4$(x=0, 0.25, 0.5, 0.75, 1) samples prepared by solution combustion method exhibited single phase cubic structure. The crystallite sizes for the sintered samples were calculated using Debye Sherrer formula and are less than 100nm, indicating that the synthesized ferrites are nano in nature. The magnitudes of lattice constant for the present samples are in the range of $8.3031A^0$ to $8.3691A^0$. The FESEM results indicate that the surface morphology of the prepared Ni^{+2}doped $CrFe_2O_4$ nano-particles are nearly spherical in shape. The frequency dependence of dielectric constant and conductivity can be understood through Maxwell-Wagner type interfacial polarization. The maximum value of ε' and σ_{ac} observed for x=0.5 composition is because of excess formation of ferrous (Fe^{+2}) ions in the system.

5. ACKNOWLEDGEMENTS

Authors are highly thankful to STIC, Cochin and CENSE, IISc-Bangalore for providing PXRD and FESEM facilities to accomplish this research work.

REFERENCES

Akhtar M.N, Yahya N, Koziol K, Nasir N, Synthesis and characterizations of $Ni_{0.8}Zn_{0.2}Fe_2O_4$-MWCNTs composites for their application in sea bed logging, Ceram.Int, 37, 2011, 3237-3245.

Akhtar M.N, Yahya N, Sattar A, Ahmad M, Investigations of structural and magnetic properties of nanostructured $Ni_{0.5+x}Zn_{0.5-x}Fe_2O_4$ based magnetic feeders for CSEM Application, Int.J.Appl.Ceram.Technol, 1, 2014, 1-13.

Aphesteguy J.C, Damiani A, DiGiovanni D, Microwave absorbing characteristics of epoxy resin composites containing nanoparticles of Ni-Zn and NiCuZn-ferrites. Physica B: condensed Matter, 404 (18), 2009, 2713-2716.

Atif M, Nadeem M, Grossinger R, Studies on the magnetic, magnetostrictive and electrical properties of Sol-gel synthesized Zn doped nickel ferrite, Journal of Alloys and Compounds, 509 (18), 2011, 5720-5724.

Azadmanjari J, Salehani H K, Barati M.R, Preparation and electromagnetic properties of $Ni_{1-x}Cu_xFe_2O_4$ nano-particles ferrite by solgel auto-combustion method, Materials Letters, 61 (1), 2007, 84-87.

Azadmanjiri J, Structural and electromagnetic properties of Ni-Zn ferrites prepared by sol-gel combustion method, Materials chemistry and physics, 109 (1), 2008, 109-112.

Brabers V.A.M, Progress in spinel ferrite research, Handbook of Magnetic Materials, 8, North-Holand, Amsterdam, 1995, 189-324.

Costa A.C.F.M, Lula R.T, Kiminami R, Preparation of nanostructured $NiFe_2O_4$ catalysts by Combustion reaction, Jour.Material science, 41 (15), 2006, 4871-4875.

De Biasi R.S, Figueiredo A.B.S, Fernandes A.A, Synthesis of cobalt ferrite nanoparticles using combustion waves, Solid State Communications, 144 (1-2), 2007, 15-17.

Gou L, Shen X, Meng X, Effect of Sm^{3+} ions doping on structure and magnetic properties of nanocrystalline $NiFe_2O_4$ fibers, Journal of Alloys and Compounds, 490 (1-2), 2010, 301-306.

Guo X, Qiy, Li X, Preparation, characterization and photo catalytic properties of nano-meter $ZnFe_2O_4$, Journal of University of Science and Technology Beijing, 11 (5), 2004, 474-476.

Gupta N, Verma A, Kashyap S.C, Dielectric behavior of spin deposited nano-crystalline nickel-zinc ferrite thin films processed by citrate-route, Solid State Communications, 134 (10), 2005, 689-694.

Hankare P.P, Patil R.P, Garadkar K.M, Synthesis, dielectric behavior and impedance measurement studies of Cr-substituted Zn-Mn ferrites, Mater.Res.Bull, 46, 2011, 447.

Kambale R.C, Adhate N.R, Chougule B.K, Magnetic and dielectric properties of mixed spinel Ni-Zn ferrites synthesized by citrate –nitrate combustion method, Journal of Alloys and compounds, 491 (1-2), 2010, 372-377.

Maxwell JC, Electricity and Magnetism, Vol 1, Oxford University Press, Oxford, 1929.

Selvan R.K, Augustin C.O, Berchmancs L.J, Combustion synthesis of $CuFe_2O_4$, Materials Research Bulletin, 38 (1), 2003, 41-54.

Shukla R, Ningthoujam R.S, Umare S.S, Decrease of super paramagnetic nature at room temperature in ultrafine $CoFe_2O_4$ particles by Ag doping, Hyperfine Interactions, 184 (1-3), 2008, 217-225.

Sutka A, Stingaciu M, Mezinskis G, An alternative method to modify the sensitivity of p-type $NiFe_2O_4$ gas sensor, Journal of Materials Science, 47 (6), 2012, 2856-2863.

Vijaya Bhaskar Reddy P, Ramesh B, Gopal Reddy C, Electrical conductivity and dielectric properties of Zinc substituted Lithium ferrites prepared by Sol-gel method, Physics B: Condensed Matter, 405 (7), 2010, 1852-1856.

Wagner KW, Ann Phys, 40:817, 1913.

Waqas H, Qureshi A.H, Influence of pH on nano-sized Mn-Zn ferrite synthesized by Sol-gel auto combustion process, Journal of Thermal Analysis and Calorimetry, 98 (2), 2009, 355-360.

Yao C, Zeng Q, Goya G.F, Torres T, $ZnFe_2O_4$ nanocrystals: Synthesis and magnetic properties, J.Phys.Chem, 111, 2007, 12274.

Yue Z, Zhou J, Li L, Synthesis of nanocrystalline NiCuZn ferrite powders by sol-gel auto-combustion method, Journal of magnetism and magnetic materials, 208 (1), 2000, 112.